극저사이클 하중하에서 강구조 부재의 비선형 유한요소해석

Non-linear Finite Element Analysis of Steel Members under Very-Low-Cycles of Loading

朴 鍊 洙*
Park, Yeon Soo

요 약

본 수치해석의 목적은 앵글 강부재의 극저사이클 파괴실험으로부터 얻어진 거동의 재현 및 특히, 부재중에서 가장 심한 응력을 받는 부분에 대한 국소 응력-변형률의 이력과 누적상황을 추적하는 것이다. 이를위해, 범용 구조해석 프로그램인 MSC/NASTRAN을 이용하여, 재료 및 기하학적 비선형을 고려한 대변형 3차원 유한요소해석을 행하였다. 해석은 2단계 즉, 해석 Ⅰ과 Ⅱ로 나누어 실시하였으며, 본 해석의 전반적인 거동은 실험결과와 매우 잘 일치하였다.

Abstract

The objective of this numerical analysis is to trace the hysteretic behavior of steel angles under very-low-cycle loading test, especially the history and cumulative state of local stress-strain at their critical parts. The computer model is based on a three-dimensional, non-linear analysis by using the finite element program, MSC/NASTRAN, which includes the effects of the material and geometric non-linearities. The analysis was performed as two stage procedures, namely Analysis Ⅰ and Ⅱ. The overall behavior from this analysis showed good agreement with the experiment.

INTRODUCTION

To determine quantitative relationships among the important physical factors causing cracks and rupture of steel members due to strong cyclic excitations as in destructive earthquakes, the authors conducted the tests on failure under very-low-cycle loading[1-3]. In general, however, it is extremely difficult to trace the plastic local strain over 3% through experiments, because of adhesive properties' problems between the surface of specimen and strain gages under very-low-cyclic loading conditions. The use of the numerical analysis mak-

* 正會員 · 日本 京都大學 防災研究所 都市耐震센터 공동연구원

이 논문에 대한 토론을 1994년 12월 31일까지 본 학회에 보내주시면 1995년 6월호에 그 결과를 게재하겠습니다.

es it possible to simulate the local strain history. The main objective of this numerical analysis is to simulate the hysteretic behavior of steel angles under very-low-cycle of loading, especially the history and cumulative state of local strain at their critical parts. This is a finite element method tracing toward cracking of steel members under cyclic loads such as an earthquake.

Under severe cyclic deformations as in a strong earthquake, the responses of structures are usually in nonlinear range. Most of structural steel members often continue to deform in the post-buckling range with local deformation. Classical formulations of this post-buckling behavior[4-7] lead to a set of partial differential equations which were characterized by a coupling of the dependent variables describing the in-plane and out-of-plane behavior of the plate. It was difficult or very formidable to solve the equations. Theoretical analysis, therefore, based on classical formulation needs to be simplified in these differential equations. This simplification results in no good representation to local behaviors of plate elements in the elasto-plastic members under repeated loadings. The finite element method considering material and geometric nonlinearities is now available as an alternative approach to such problems with the rapid developments in computer hardware and software[8].

MSC / NASTRAN is the finite element computer program for structural analysis developed by the National Aeronautics and Space Administration(NASA) that is intended for general use[9,10]. The nonlinear capabilities of static analysis are provided as self-contained solution sequence SOL66 of MSC / NASTRAN. Namely, the solutions of the nonlinear analysis are obtained from a trial-and-error search procedure, search / iteration / increment strategy, for the incremental loading steps. The search procedure starts from a particular stress and position state and terminates when the basic equations are satisfied within a known tolerance. This analysis was made by using the solution sequence SOL66 in Version 66 of MSC / NASTRAN. All computer works have been made on the FUJITSU M-1800 / 30 computer system of Data Processing Center, Kyoto University.

PROCEDURE OF NUMERICAL ANALYSIS

The analysis was performed as two stage procedures, namely Analysis Ⅰ and Ⅱ. In the Analysis Ⅰ, in order to investigate the correlation between the mesh sizes and accuracy of response, four models having different element sizes, as shown in Fig.1, were analyzed. The optimal mesh division obtained from the Analysis Ⅰ will be used in the Analysis Ⅱ to simulate the behavioral characteristics of the elasto-plastic steel members under the very-low-cycles of loading. A total of four specimens selected from the experiments[1-3] have been modeled in the Analysis Ⅱ.

FINITE ELEMENT MODELING

The three-dimensional coordinate system of finite element model used in the Analysis Ⅰ and Ⅱ is shown in Fig. 2 for the angle L-40×40×3 or L-40×40×5. The 4-noded quadrilateral isoparametric shell elements(QUAD4 elements) were used in modeling the tested part of the angle specimen. The material property in this analysis has been assumed to be bilinearly elasto-plastic with kinematic hardening. The yield stress σ_y, Young's modulus E_S and Poisson's ratio ν were taken to be 349 N / mm^2, 2.06×10^5 N / mm^2 and 0.3, respectively.

The slope E_t, in the strain hardening region, of the stress-strain curve was selected at 1% of E_S. The von Mises yield criterion was used. Both ends of the test specimen were modeled as simply supported. Both end-supporting parts of the specimen by holding the blocks[1-3] were modeled by using the 3-noded stiff shell elements and the stiff QUAD4 elements for providing rigid-body motion in the vicinity of ends. Namely, the Young's modulus, E_S, used in the stiff QUAD4 and TRAI3 elements near the both end-supporting parts of the model was 1.37×10^3 kN / mm^2. As for the degrees of freedom, only the in-plane rotation was constrained in all the nodes of the model.

ANALYSIS Ⅰ : EFFECTS OF MESH SIZES ON MEMBER BEHAVIOR

In the Analysis Ⅰ, the monotonic loading up to the prescribed displacement with contractive global strain of 8% was programmed. The model in the Analysis Ⅰ had 154, 230, 306 and 466 shell elements(see Fig. 1). The computed relationships between the load and relative axial displacement of the loading point is given in Fig. 4 for the four models. Here the load P and relative displacement Δ are normalized by the yield load N_y and length ℓ, respectively. Regardless of the mesh sizes, there is very good agreement at the values of buckling load P_{cr}. However, in the descending branch of load-axial displacement relations, large differences appear between the coarse meshes(154 & 230 elements) and fine meshes(306 & 466 elements). The reason may be that the refinement of meshes such as 306 and 466 elements causes the angle model to become flexible at the local buckling region and to produce more realistic response curves consequently. From Fig. 4, it appears that the 306 mesh solution is in excellent agreement with the results for the finest 466 model. The model with 306 meshes, therefore, is selected as an optimal model to

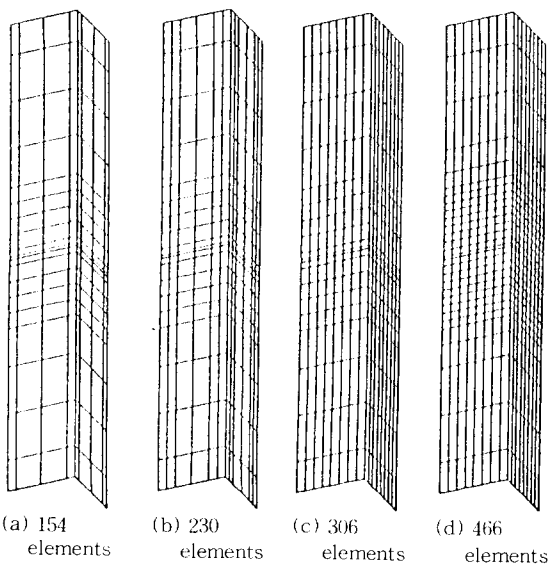

Fig. 1 Mesh division to investigate effects of element sizes.

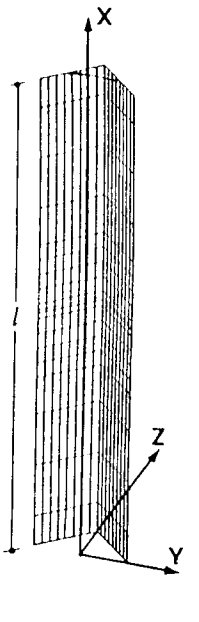

Fig. 2 Typical model

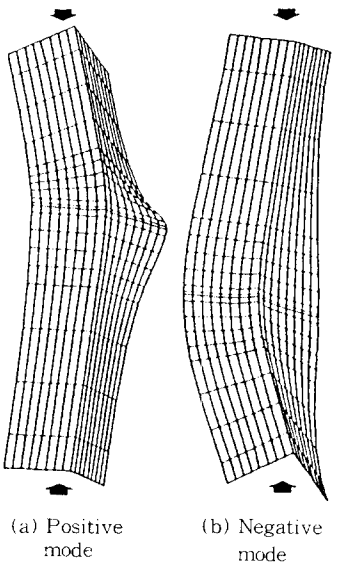

Fig. 3 Deformed shapes at $\Delta/\ell = -0.08$

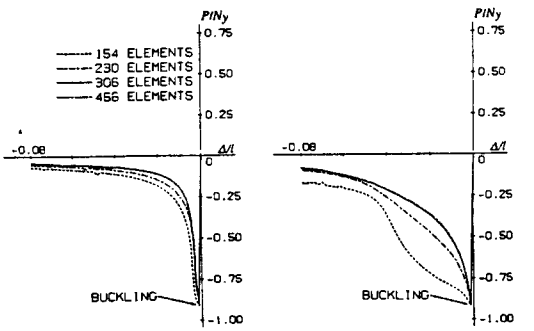

(a) Positive deflection mode (b) Negative deflection mode

Fig. 4 Comparison of load-axial displacement relations

represent the experimental behaviors of angles under very-low-cycle loading. Thus, the model in the Analysis Ⅱ comprised the 306 shell elements.

ANALYSIS Ⅱ : TRACING EXPERIMENTAL BEHAVIOR

The models in the Analysis Ⅱ were subjected to cyclically enforced displacement, in the contraction side(L3CP[1,2] and L5CP[1,2] mod-

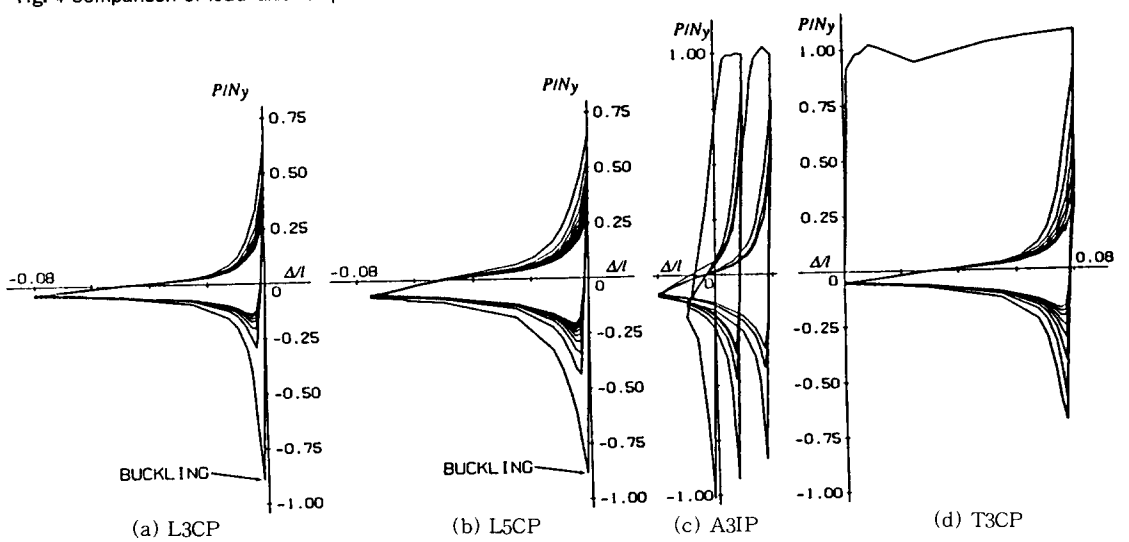

(a) L3CP (b) L5CP (c) A3IP (d) T3CP

Fig. 5 Load-axial displacement relations[Analysis]

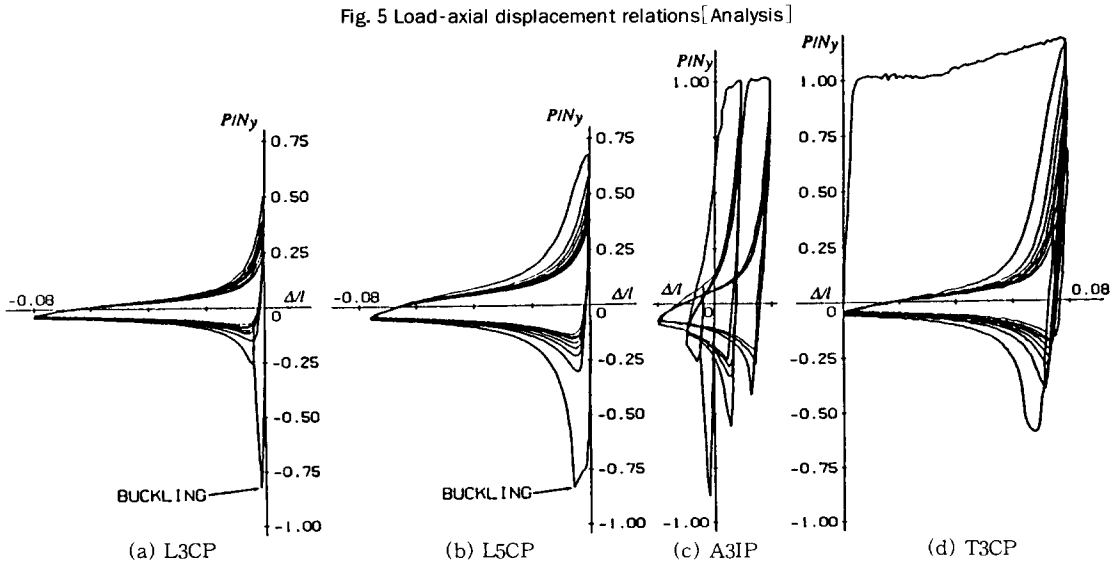

(a) L3CP (b) L5CP (c) A3IP (d) T3CP

Fig. 6 Load-axial displacement relations[Experiment]

els) and elongation side(T3CP[3] model) with a constant amplitude 8% of the length ℓ or in the alternate side(A3IP[3] model) with an increased displacement amplitude. The load was applied with small eccentricities, about 0.2 -1.0mm distant from the gravity center at each end, in the Z-direction(Fig. 2), in order to produce a desired deflection mode as observed in the experiment, as shown in Fig. 3. The analysis was basically performed up to the number of cycles where outbreak and / or penetration of cracks through the thickness of the angle leg were observed in the experiment. Each model for the Analysis II required about 3 hours of CPU time on the average.

GLOBAL AND LOCAL DEFORMATIONS

Fig. 3 shows the three-dimensional views of global deformation obtained from the analysis at stage $\Delta / \ell = -0.08$ in the first cycle. In the case of the positive deflection mode(Fig. 3(a)), global buckling was accompanied by large local deformation at the mid-height portion. This local deformation was accumulated with increasing number of cycles after global buckling took place. The most severe deformation occurred at the edge elements of the mid-height cross-section. In the case of negative mode(Fig. 3(b)), however, global buckling deformation was obtained in early stages of the first compressive loading and the most significant stress concentration was observed at the corner elements near the leg joint of the mid-part.

AXIAL LOAD-DISPLACEMENT RELATIONS

A comparison is made in Figs. 5 and 6 for the dimensionless load-axial displacement curves from the analysis and experiment. The analytical overall behaviors show good agreement with the experimental results. In the case of constant displacement loading started from the contraction side(see(a) and (b) in Figs.5 and 6), the compressive load decreased suddenly after the global buckling occurred at an early stage of the first cycle due to the inelastic local buckling. The compressive load-carrying capacities at each cycle after the first cycle were significantly deteriorated, but only a small decrease was seen in the succeeding tensile load-carrying capacities. The fairly higher compressive strength in the second cycle at each amplitude level under the alternately increased displacement loading(A3IP model) was calculated by the numerical analysis, as indicated in Fig. 5(c). This phenomenon may be attributed to the compressive loading for the nearly straight model regained by pure tensile yielding after being plastically deformed into a crooked configuration. In the case of cyclic loading started from a tensile displacement(Fig. 5(d)), the compressive strength in the first cycle was reduced considerably by the Bauschinger effect and the residual crookedness due to the eccentric tensile loading.

TRACING OF LOCAL STRAIN HISTORY

Figs. 7 and 8 show the axial stress-strain hysteresis and the plastic local strain history, respectively, on the inner and outer surfaces of the edge elements of the mid-height cross-section. The analytical results show that the maximum absolute local strain in the first cycle was in the range of 24−26% in the L3CP and L5CP model where loading was started in the contraction side, 13% in A3IP with the increased displacement loading, and about 40% in T3CP, which started from the elongation side. The maximum absolute strain in the loading cycle, in which the first crack took place

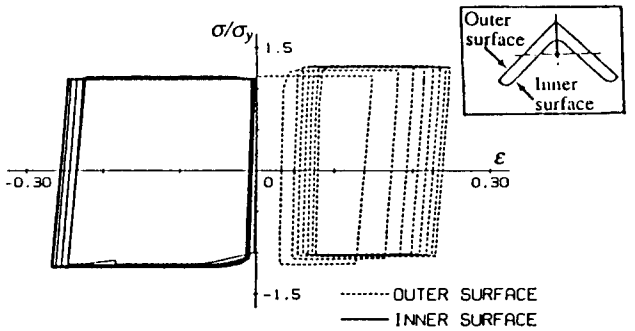

(a) L3CP

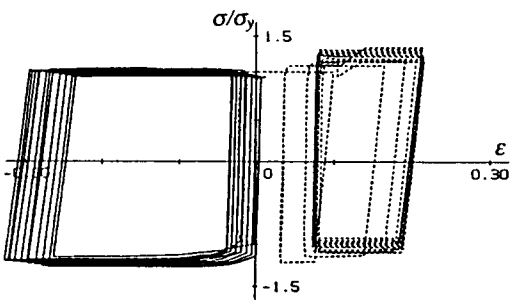

(b) L5CP

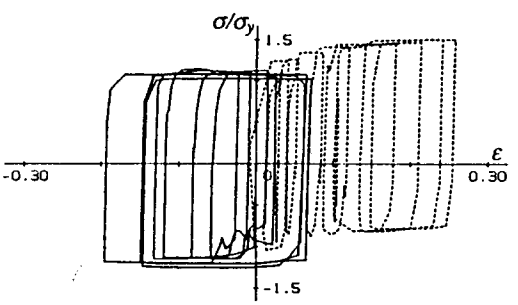

(c) A3IP

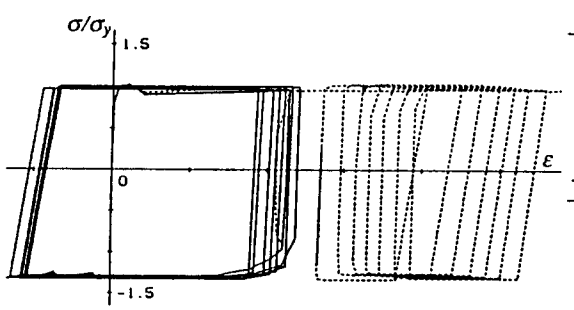

(d) T3CP

Fig. 7 Local stress-strain hysteresis[Analysis]

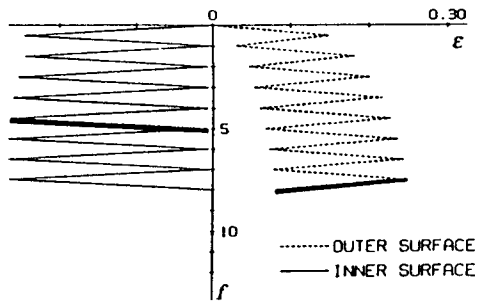

(a) L3CP

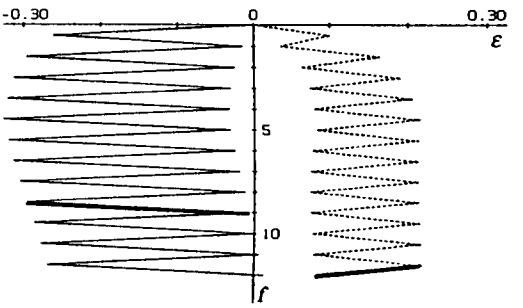

(b) L5CP

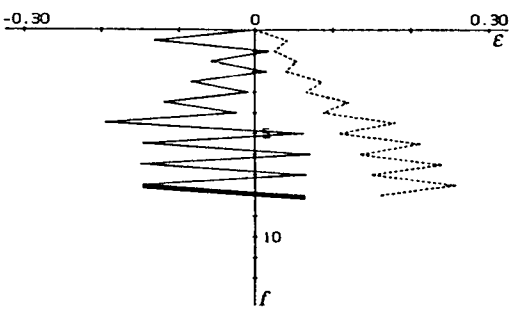

(c) A3IP

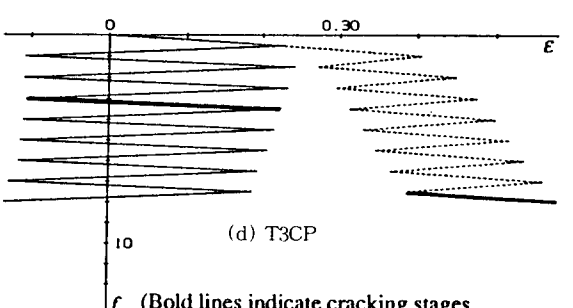

(d) T3CP

(Bold lines indicate cracking stages in the corresponding testing.)

Fig. 8 Local strain histories with the increasing number of cycles[Analysis]

indicated by bold lines in Fig. 8, was of the order of 27−30% in the cases of L3CP and L5CP, 26% in A3IP, and 50% in T3CP.

As shown in Fig. 8, the amplitudes of local strain on the inner surface of the critical elements were approximately 10−40% in the first cycle. This indicate that the angle model under the very-low-cycle loading have partially experienced very large strain with inelastic local buckling. In the cases of constant displacement loading(see Fig.8(a), (b) and (d)), a small change of the amplitudes of plastic strain component per each cycle was observed such as a fatigue behavior. Regardless of the loading history, the strain amplitudes on the inner surface is larger than the outer surface results. Namely, the most severe concentration of local deformation occurs at the inner surface of the edge elements of the mid-height portion. This is clearly related to the phenomenon of the first cracking on the concave side of the overall buckling deformation, as observed experimentally.

A trial computation was made for the summation of plastic component of strain in the tensile stress side in each cycle, up to the outbreaks of cracks. This attained the values of about 100−250%, irrespective of the loading patterns. These numbers correspond to the residual local strain of about 100%[1-3] at the ruptured portion under the monotonic-tensile testing. This sum, therefore, might be an indicator to represent the accumulated damage due to very-low-cycle loading.

CONCLUDING REMARKS

The results of a numerical analysis by the FEM program were presented for steel angle members under very-low-cycle of loading. The overall behavior from the analysis shows good agreement with the experiment. The local strain history at the critical section was traced for large cyclic deformation by the numerical analysis. Under the very-low-cycles of loading, the angle model have partially experienced very large strain with inelastic local buckling. The most severe concentration of local deformation occurs on the concave surface of the overall buckling deformation.

REFERENCES

1. Y.-S. Part, S. Iwai, T. Nonaka and H. Kameda, "Experimental Study on Structural Failure of Steel Angle Members due to Very Low Cycle Fatigue under Earthquake Loading", *Proc. of the 21st JSCE Earthquake Engineering Symposium*, Japan Society of Civil Engineers, No.125, pp.481−484, Tokyo, Japan, July 1991.
2. Y.-S. Park, S. Iwai, T. Nonaka and H. Kameda, "Tests on Failure of Angles under Very Low Cycles of Loading", *Proc. of the 1st KAIST-National Taiwan University-Kyoto University Tri-lateral Seminar/Workshop on Civil Engineering*, Kyoto, Japan, pp.53−56, Nov. 1991.
3. S. Iwai, Y.-S. Park, et al., "Tests on Very Low-Cycle Fatigue of Steel Members subjected to Reversed Displacement Loading", *Proc. Annual Conference of Kinki Branch of AIJ*, 1993(in Japanese).
4. D.O. Brush and B.O. Almroth, *Buckling of Bars, Plates, and Shells*, McGraw-Hill Book Company, 1975.
5. R. Szilard, *Theory and Analysis of Plates-Classical and Numerical Method*, Prentice-Hall, Inc., 1974.
6. S.P. Timoshenko and S. Woinowsky-Krieger, *Theory of Plates and Shells*, McGraw-Hill Book Company, 1959.
7. A.C. Ugural, *Stresses in Plates and Shells*, McGraw-Hill Book Company, 1981.
8. H. Kardestuncer, D.H. Norrie, et al., *Finite Element Handbook*, McGraw-Hill Book Company, 1987.

(접수일자 : 1993. 10. 11)